Cerebral Cortex September 2006;16:1338-1348
doi:10.1093/cercor/bhj075
Advance Access publication November 23, 2005

Neural Correlates of the Spontaneous Phase Transition during Bimanual Coordination

Yu Aramaki[1,2], Manabu Honda[1,3,5], Tomohisa Okada[1] and Norihiro Sadato[1,2,4]

[1]Department of Cerebral Research, National Institute for Physiological Sciences, 38 Nishigonaka, Myodaijicho, Okazaki, Aichi 444-8585, Japan, [2]Research Institute of Science and Technology for Society and [3]Solution Oriented Research for Science and Technology, Japan Science and Technology Agency, Kawaguchi, Saitama 332-0012, Japan, [4]Department of Functional Neuroimaging, Faculty of Medical Sciences, University of Fukui, Fukui 910-1193, Japan, and [5]Department of Cortical Function Disorders, National Institute of Neuroscience, National Center for Neurology and Psychiatry, Tokyo 187-8502, Japan

Repetitive bimanual finger-tapping movements tend toward mirror symmetry: There is a spontaneous transition from less stable asymmetrical movement patterns to more stable symmetrical ones under frequency stress but not vice versa. During this phase transition, the interaction between the signals controlling each hand (cross talk) is expected to be prominent. To depict the regions of the brain in which cortical cross talk occurs during bimanual coordination, we conducted event-related functional magnetic resonance imaging using a bimanual repetitive-tapping task. Transition-related activity was found in the following areas: the bilateral ventral premotor cortex, inferior frontal gyrus, middle frontal gyrus, inferior parietal lobule, insula, and thalamus; the right rostral portion of the dorsal premotor cortex and midbrain; the left cerebellum; and the presupplementary motor area, rostral cingulate zone, and corpus callosum. These regions were discrete from those activated by bimanual movement execution. The phase-transition–related activation was right lateralized in the prefrontal, premotor, and parietal regions. These findings suggest that the cortical neural cross talk occurs in the distributed networks upstream of the primary motor cortex through asymmetric interhemispheric interaction.

Keywords: bimanual coordination, fMRI, interhemispheric interaction, spontaneous phase transition

Introduction

The human body has a large number of degrees of freedom. However, these are limited by neural constraints, as well as muscular and perceptual influences on pattern stability. For example, patterns of bimanual coordination in which homologous muscles are active simultaneously are more stable than those in which homologous muscles are engaged in an alternating fashion (egocentric constraint; Swinnen and others 1997). This is demonstrated dramatically by the phase transition during bimanual movement: If a subject performs a movement in the asymmetrical mode, increasing the movement frequency ultimately results in a phase transition toward the more stable mirror-symmetrical mode, but the opposite transition does not occur (Kelso 1984). This bimanual interaction was first formalized theoretically at the behavioral level by dynamic systems theory (Haken and others 1985; Schöner and Kelso 1988). While investigating this phase transition from the "unstable" to the stable phases of the bimanual finger-tapping task, Meyer-Lindenberg and others (2002) demonstrated the neuronal dynamics conforming to the predictions made by the nonlinear system theory. First, using positron emission tomography, they depicted the cortical regions related to the degree of behavioral instability, assuming that these unstable areas increase their neural activities as the frequency of the movement increases. Within these areas, they found that a minor disruption by double-pulse transcranial magnetic stimulation to the right dorsal premotor cortex (PMd) evoked large-scale phase transitions in participants' performances.

As well as dynamic systems theory, several theoretical models have been proposed to formalize the process of bimanual coordination (de Oliveira 2002). First, the strong tendency toward spatiotemporal similarity in bimanual movements has led to the proposal that a common motor plan exists for both limbs within the framework of generalized motor programs (GMPs; Schmidt 1975) that specify the entire "shape" of a movement even before its execution begins. By contrast, the concept of intermanual cross talk maintains that 2 independent motor plans exist (Marteniuk and MacKenzie 1980). Interactions between the movements of the 2 arms are assumed to result from cross talk at multiple levels between the signals controlling the 2 arms. The lowest level of cross talk supposedly occurs downstream from the specification of movement parameters, possibly through the ipsilateral corticospinal tract (Cattaert and others 1999). Although each hand is mainly controlled by the contralateral hemisphere, there is also an ipsilateral influence that is integrated with the contralateral one. This ipsilateral influence alters the muscular activation, and as a result, the movement that each arm performs becomes slightly similar to the movement of the opposite arm (Carson 2005). In addition, cross talk might also occur at a higher level because the neural population coding in the parietal, premotor, and primary motor cortices (M1) corresponds to the direction of movement of the contralateral hand (Georgopoulos and others 1986; Kalaska and others 1997; Kakei and others 1999). Thus, a combined GMP/cross-talk model is possible. In such a combined model, the GMP might be created at a hierarchically higher level than the programs for the 2 arms, providing a functional scheme that has traits of both 1 common and 2 separate motor plans.

The cross-talk model successfully formalized the spontaneous phase transition. Cattaert and others (1999) replicated the spontaneous phase transition in cyclical movements using a cross-talk model simulation in which a percentage of the force command is dispatched to the other limb. However, the neural substrates underlying the phase transition are as yet unknown.

The aim of the present study was to delineate the neural substrates of bimanual interaction during the spontaneous phase transition using event-related functional magnetic resonance imaging (fMRI). Within the framework of the cross-talk model, the moment of the phase transition from the parallel to mirror mode is regarded as cross talk. Because the synaptic firing rate increases as the system nears the transition point (Rose and Siebler 1995), the collective change in neural activity during the spontaneous phase transition is expected to represent the locations where the cortical neural cross talk primarily occurs.

Our hypothesis was that the spontaneous phase transition might be represented by bihemispheric asymmetrical neural substrates upstream of M1. We have several reasons for this prediction. First, interhemispheric interaction through the corpus callosum (CC) is related to the spontaneous phase transition from the stable to the unstable mode. Kennerley and others (2002) investigated the role of the CC in spatial coupling during continuous bimanual circle drawing. Spatial coupling is inferred by the reduced stability observed when the circles are produced asymmetrically (nonhomologous movements) compared with when the movements are symmetrical (homologous movements). In the asymmetric condition, the control participants showed occasional phase transitions toward the more stable symmetric mode. By contrast, the callosotomy patients were equally likely to exhibit phase transitions in the symmetric condition as in the asymmetric condition. Hence, it is expected that the neural substrates of the spontaneous phase transition will be distributed in both hemispheres as a result of interhemispheric interaction. Second, in the bimanual circle-drawing task, the reversal in direction during the antiphase mode was partly associated with the nondominant hand (Walter and Swinnen 1992; Byblow and others 1994, 1998, 2000; Sherwood 1994; Semjen and others 1995; Treffner and Turvey 1995; Rogers and others 1998; Garry and Franks 2000), suggesting asymmetry in the neural substrates of cross talk. Lastly, clinical and imaging studies have indicated left-hemisphere dominance in the representation of motor skill (Sirigu and others 1996; Haaland and others 2000), including that of bimanual coordination (Serrien and others 2001). Based on a functional scheme that has traits of both 1 common and 2 separate motor plans, neural cross talk is expected to be asymmetrical.

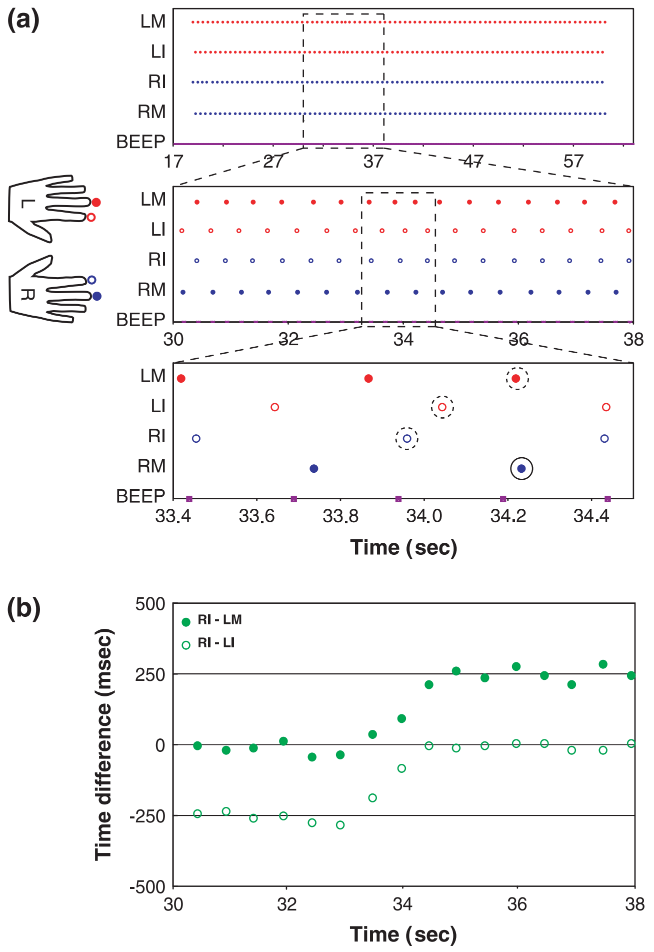

Figure 1. (*a*) Time sequence of the bimanual finger-tapping data during the fMRI experiment at different timescales, with wide (top; 40 s), medium (middle; 8 s), and narrow (bottom; 1 s) ranges around the phase transition. Open red, closed red, open blue, and closed blue symbols show the left index, left middle, right index, and right middle fingers, respectively. Dashed and solid circles show the phase-transition time of each finger as denoted in Materials and Methods. We selected the first time point (solid circle) as the phase-transition time of the trial. (*b*) Tapping-time differences between the RI and the corresponding LM finger (closed green circle) and between the RI and the corresponding LI finger (open green circle) in the medium range timescale (8 s) around the phase transition.

Materials and Methods

Participants

Fifteen subjects (age range, 24–31 years; mean ± SD, 26.7 ± 2.12 years; 9 men and 6 women) participated in this study. The subjects were all right handed according to the Edinburgh Handedness Inventory (Oldfield 1971). The mean handedness score was 0.92 ± 0.09 (mean ± SD). The protocol was approved by the ethical committee of the National Institute for Physiological Sciences, Japan. All subjects gave their written informed consent for the study.

Magnetic Resonance Imaging

A time course series of 400 volumes was acquired in 1 session using T_2*-weighted gradient echo-planar imaging (EPI) sequences with a 3.0-T magnetic resonance (MR) imager (Allegra; Siemens, Erlangen, Germany). Each volume consisted of 26 axial slices with a slice thickness of 6 mm and no gap, which included the entire cerebral cortex and cerebellum. The time interval between 2 successive acquisitions of the same image was 1500 ms, and the echo time was 30 ms (flip angle, 70°). The field of view was 192 mm, and the in-plane matrix size was 64 × 64 pixels, with a pixel dimension of 3 × 3 mm.

For anatomical reference, T_1-weighted images were obtained from each subject with location variables identical to those of the EPIs. In addition, three-dimensional (3D) high-resolution T_1-weighted images (magnetization-prepared rapid acquisition in gradient echo [MPRAGE]) were obtained. A total of 192 transaxial slices were acquired. The in-plane matrix size was 256 × 256, the slice thickness was 1 mm, and the pixel size was 0.898 × 0.898 mm.

Tasks

Subjects performed the bimanual rhythmic finger-tapping task using their index and middle fingers (Fig. 1). Two USB magnetic resonance imaging (MRI)–compatible 10-key pads (TK-UYGT, ELECOM, Osaka, Japan) connected to a personal computer (Dimension 8200; Dell Computer Co., Texas) were used to record the finger taps. For right-handed finger taps, the keys “1” (for the index finger) and “3” (for the middle finger) of the 10-key pad were used. For the left hand, the keys “7” (for the index finger) and “9” (for the middle finger) of another 10-key pad were pressed. We defined 2 coordination modes in the present study: the “mirror” and “parallel” modes. The mirror mode was defined as the synchronous tapping of both index fingers alternating periodically with the synchronous tapping of both middle fingers: (_I × I_), (M_ × _M), (_I × I_), and so on. The parallel mode was defined as the synchronous tapping of the left middle and right index fingers, which alternated periodically with the synchronous tapping of the left index and right middle fingers: (M_ × I_), (_I × _M), (M_ × I_), and so on (Mechsner and others 2001).

It is well known that the phase transition from the parallel to the mirror mode is frequency dependent: the faster the movement, the earlier the mode conversion occurs (Kelso 1984). Because the aim of this study was to investigate the state-related brain activity (i.e., in the parallel vs. mirror mode) as well as the phase-transition–related activity, we set the movement frequency so that the subjects could maintain the parallel mode for more than 10 s. Prior to the fMRI experiment, the subjects were trained to perform auditory-cued (260 Hz and 50 ms) bimanual rhythmic-tapping tasks in a supine position. Auditory cues were provided by Presentation software (Neurobehavioural Systems, Albany, California), which was also used to record the timing of the key presses. The subjects were required to gaze at the fixation point and, hence, could not see their own hands. The subjects always began with the parallel mode. The instructions to the subjects emphasized that when the phase transition from the parallel to the mirror mode occurred, they should maintain the mirror-mode movements. We set 5 different levels of movement frequencies, ranging from 2 to 4 Hz or from 3 to 5 Hz at 0.5-Hz increments, in order to determine the frequency at which each subject made the spontaneous phase transition from parallel to mirror mode after 10–20 s. Subjects performed 10 trials at each frequency. If more than 1 frequency level passed the criterion, we used the highest frequency for the fMRI experiment.

Functional Magnetic Resonance Imaging

In the fMRI experiment, the subjects underwent the same auditory-cued bimanual rhythmic-tapping tasks in a supine position. To minimize head motion, we used tight but comfortable foam padding placed around the subject's head. A liquid crystal display projector (DLA-M200L; Victor, Yokohama, Japan) located outside and behind the scanner projected a crosshair fixation point through another waveguide to a translucent screen, which the subject viewed via a mirror attached to the head coil of the MRI scanner. Similar to the practice condition, the subjects were required to fixate the crosshair on the screen and, hence, could not see their own hands. The subjects' hands were placed on the 10-key pads connected to a personal computer to record their responses. The predetermined frequency of the cued movement was 3.8 ± 0.62 Hz (mean ± SD), which varied across the subjects. Auditory cues were provided by the Presentation software, which was also used to record the timing of the key presses. Each subject started the parallel movement when the experimenter touched their foot. The experimenter carefully monitored the finger movements of the subject to detect any sudden changes in the coordination patterns. Approximately 20 s after the transition, the experimenter touched the foot of the subject to signal them to terminate the movement. The next trial started approximately 20 s after the termination of the previous trial. Between 7 and 10 trials were repeated during each 10-min session. The auditory cue was provided continuously throughout the scanning session. The session was repeated four times for each subject. Instructions to the subject emphasized that their task was to keep up with the pacing signal and that if an involuntary switch from the parallel to the mirror pattern occurred, they should maintain the mirror pattern.

Behavioral Data Analysis

Definition of the Time of Phase Transition

In this study, we defined the point at which the phase transition occurred as follows. If the subject maintained the mirror mode, the timing of the key press of the right index finger would be closer to that of the key press of the left index finger than that of the left middle finger. The following inequality should therefore be fulfilled:

$$\min(|\mathrm{RI}(i)-\mathrm{LM}|)>\min(|\mathrm{RI}(i)-\mathrm{LI}|). \qquad (1)$$

Here, $\mathrm{RI}(i)$ is the time of the i-th key press of the right index finger, and LM and LI are vectors of all the key-press times of the left middle and index fingers, respectively. Therefore, the first time point ($\min \mathrm{RI}(i)$) fulfilling equation (1) can be considered the transition time (T) of the right index finger from the parallel to the mirror mode. A similar calculation was performed for the other 3 fingers in order to define the discrete time series of each ($\mathrm{RM}(j)$, $\mathrm{LI}(k)$, and $\mathrm{LM}(m)$):

$$\min(|\mathrm{RM}(j)-\mathrm{LI}|)>\min(|\mathrm{RM}(j)-\mathrm{LM}|), \qquad (2)$$

$$\min(|\mathrm{LI}(k)-\mathrm{RM}|)>\min(|\mathrm{LI}(k)-\mathrm{RI}|), \qquad (3)$$

$$\min(|\mathrm{LM}(m)-\mathrm{RI}|)>\min(|\mathrm{LM}(m)-\mathrm{RM}|). \qquad (4)$$

For the right index finger, $\min \mathrm{RM}(i)$, $\min \mathrm{LI}(k)$, and $\min \mathrm{LM}(m)$ were defined as the T values of the right middle, left index, and left middle fingers, respectively. The T value was defined as the latest T among the 4 fingers (Fig. 1):

$$T=\max(\min\mathrm{RI}(i),\min\mathrm{RM}(j),\min\mathrm{LI}(k),\min\mathrm{LM}(m)). \qquad (5)$$

Calculation of Behavioral Asymmetry in the Phase Transition

At the phase transition, irregularities should be observed in the intertap intervals of both or either hands. Previous behavioral studies have reported how the nondominant hand contributes to the phase transition (Semjen and others 1995; Kennerley and others 2002). If the nondominant hand (the left hand in our subjects) tends to be entrained by the dominant (right) one, the variance of the intertap interval of the nondominant hand around the phase transition should be greater than that of the dominant hand. Hence, we used the ratio of the fluctuation of the intertap interval of each hand around the phase transition to evaluate the asymmetric contribution of each hand to the phase transition. Using 4 points around the T value (the nearest point, 2 points before, and 1 point after), the deviation of the intertap interval of each finger from the ideal intertap interval (twice the interbeep interval) was calculated (dev(RI) and dev(LI), in which RI and LI refer to the right and left index fingers, respectively). The laterality index was calculated as follows:

$$\text{Laterality index}=\left\{\sum(\mathrm{dev}(\mathrm{RI}))^2-\sum(\mathrm{dev}(\mathrm{LI}))^2\right\}/\left\{\sum(\mathrm{dev}(\mathrm{RI}))^2+\sum(\mathrm{dev}(\mathrm{LI}))^2\right\}. \qquad (6)$$

The laterality index can range from −1 to 1; a positive value indicates that near the phase transition the fluctuation of the intertap interval of the right index finger is larger than the left and vice versa. We calculated the laterality index for every trial and averaged all the trials for each subject. Tapping data from the index fingers are presented here. Analyses were also performed on data from the other fingers with similar results.

fMRI Data Analysis

The first 6 volumes of each fMRI session were discarded due to unsteady magnetization, and the remaining 394 volumes per subject were used for the analysis. The data were analyzed using statistical parametric mapping (SPM99; Wellcome Department of Cognitive Neurology, London, UK) (Friston, Ashburner, and others 1995; Friston, Holmes, and others 1995) implemented in Matlab (Mathworks, Sherborn, Massachusetts). Following the slice-timing correction (Buchel and Friston 1997) and realignment of the fMRI data, the 3D high-resolution T_1-image was coregistered to the fMRI data using the anatomical T_1-weighted image with identical locations to the fMRI data. The parameters for affine and nonlinear transformation into the standard stereotaxic space (Montreal Neurological Institute [MNI] template) (Evans and others 1994) were estimated using the 3D high-resolution T_1-image with least squares means (Friston, Ashburner, and others 1995). The parameters were then applied to the realigned fMRI data. The anatomically normalized fMRI data were filtered using a Gaussian kernel of 6 mm (full width at half maximum) in the x, y, and z axes.

Statistical analysis was conducted at 2 levels. First, individual task-related activation was evaluated. Second, in order to make inferences at the population level, individual data were summarized and incorporated into a random-effect model (Friston and others 1999).

Individual Analysis

The fMRI time series data were analyzed using a general linear model (Friston, Holmes, and others 1995). Three conditions were included: the parallel mode, the mirror mode, and the phase transition. Neuronal models for all conditions were generated in an event-related fashion: The transition was expressed as delta functions and, hence, had no duration. The parallel and mirror modes were expressed as trains of delta functions with time intervals of 0.2 s. The trains lasted for the variable duration of each activation epoch. Each neuronal model of the delta function or trains of delta functions was convolved with a predefined hemodynamic-response function. The time series of the ?MR signal of each voxel, Y, was modeled as follows:

$$Y = \text{constant} + \beta 1(\text{parallel}) + \beta 2(\text{transition}) + \beta 3(\text{mirror}) + \varepsilon. \qquad (7)$$

Here, ε is the statistical error term, and (parallel), (transition), and (mirror) are the time series of hemodynamic response to each of the respective conditions. These 3 independent variables were centered on zero. The frames from after the mirror condition to the start of the next session lasted for approximately 30 s. These frames are not accounted for in the modeled conditions as they were regarded as implicit baselines. Hence, the estimated $\beta 1$ and $\beta 3$ are measures of the state-related activation, and $\beta 2$ represents the transition-related activation. The significance of these effects was tested with the t values formed by dividing the estimated parameters ($\beta 1$, $\beta 2$, $\beta 3$) and their difference ($\beta 3 - \beta 1$) by their estimated standard deviation, with adjustment for temporal autocorrelation. These t values were calculated at each and every voxel, comprising the statistical parametric maps of SPM$\{t\}$, which were transformed to a normal distribution SPM$\{Z\}$. The statistical threshold for SPM$\{Z\}$ was set at $P < 0.05$ corrected for multiple comparisons at the cluster level with a threshold of $Z < 3.09$ (Friston and others 1996).

Group Analysis with the Random-Effect Model

The weighted sum of the parameter estimates in the individual analysis constituted contrast images that were used for the group analysis (Friston and others 1999). The contrast images obtained through individual analyses represent the normalized task-related increment of the MR signal of each subject, that is, for the parallel mode, mirror mode, parallel versus mirror conditions, and the transitions between them. A total of 15 subjects with 4 contrasts each were used for the analysis.

We also flipped the contrast image of the phase transition of each subject to evaluate the laterality of the activation map (Harada and others 2004). Asymmetric involvement of the neural substrates underlying the transition was depicted by comparing the original and flipped images in a pairwise fashion. Regional activations that were significant at $P < 0.05$ (corrected for multiple comparisons at the cluster level) were considered.

The activated foci are reported as Montreal Neurological Institute coordinates, with reference to Talairach and Tournoux (1988). The MNI coordinates were transformed to Talairach coordinates through an established formula (http://www.mrc-cbu.cam.ac.uk/Imaging/Common/mnispace.shtml).

Results

Behavioral Results

In the fMRI experiment, we obtained data from an average of 36 trials (including the spontaneous phase transition; Fig. 1) per subject for statistical analysis (mean ± SD, 36.4 ± 5.53; range, 26–46). The mean time taken to reach the phase transition across all sessions for all subjects was 18.8 ± 4.0 s (range, 13.1–27.1 s). All phase transitions observed in this study were from the parallel to the mirror mode, and once the phase transition occurred, the mirror mode was maintained until the termination of the movement in all trials. The laterality index from the behavioral data around the phase transition (see Materials and Methods) was −0.12 ± 0.045 ($P = 0.019$; 1-sample t-test). This means that the variance in the phase transition of the left-finger tapping contributed significantly more to the phase transition than that of the right finger. There was no correlation between tapping speed and the laterality index ($r = -0.179$, $P = 0.52$). The number of events for left-finger tapping within a 1-s time window around the transition did not significantly differ from that for right-finger tapping ($t = -0.164$, $P = 0.87$).

Functional Brain-Imaging Data

In the parallel mode, we found activation in the following areas: the bilateral primary sensorimotor area (SM1), putamen, thalamus, and cerebellum; the right caudal portion of the dorsal premotor cortex (PMdc), inferior frontal gyrus (GFi), and insula; the left ventral premotor cortex (PMv) and inferior parietal lobule (LPi); and the supplementary motor area (SMA), pre-SMA, and cerebellar vermis (Table 1). In the mirror mode, we found bilateral activity in the SM1 and cerebellum and in the right PMdc, left superior temporal gyrus, and SMA (Table 2). When the parallel mode was compared with the mirror mode, more prominent activation was found in the bilateral PMdc, putamen, globus pallidus, thalami, and cerebellum, the right insula, left SM1, and the SMA, pre-SMA, caudal cingulate zone (CCZ), and cerebellar vermis (Table 3). Activity related to the phase transition was observed in the following areas: the bilateral PMv, GFi, middle frontal gyrus (GFm), LPi, insula, and thalamus; the right rostral portion of the PMd (PMdr) and midbrain; the left cerebellum; and the pre-SMA, rostral cingulate zone (RCZ), and CC ($P < 0.05$ corrected at the cluster level; Table 4; Fig. 2).

The phase-transition–related activation map is clearly distinct from the parallel- and mirror-mode maps. Figure 3 illustrates this point. At the level of $z = +58$ mm, phase-transition–related activation was found in the pre-SMA and the right PMdr, whereas the state-related activation involved mainly the SMA

Table 1
Brain regions activated in the parallel contrast

Cluster P	Cluster size	Voxel Z	MNI coordinates			Side	Location	BA
			x	y	z			
<0.001	1901	6.09	32	−28	58	R	SM1	4
		5.49	30	−16	68	R	PMdc	6
<0.001	1326	5.77	−42	−28	58	L	SM1	4
		4.44	−60	4	28	L	PMv	6
		4.41	−58	−2	38	L	PMv	6/44
		3.45	−48	−38	52	L	LPi	40
<0.001	1177	5.53	0	2	64		Pre-SMA	6
		5.01	6	−8	66	R	SMA	6
		4.69	−8	−4	72	L	SMA	6
<0.001	434	4.26	56	12	14	R	GFi	44
		3.87	42	16	6	R	Insula	13
<0.001	1802	6.32	24	−4	8	R	Putamen	
		5.51	−26	−6	12	L	Putamen	
		5.1	−18	−20	8	L	Thalamus	
		5.04	14	−18	10	R	Thalamus	
<0.001	2942	5.04	22	−66	−20	R	Cerebellum	
		4.74	−26	−54	−22	L	Cerebellum	
		4.58	−2	−72	−18	L	Cerebellar vermis	

Note: $P < 0.05$ corrected at the cluster level.

Table 2
Brain regions activated in mirror contrast

Cluster P	Cluster size	Voxel Z	MNI coordinates			Side	Location	BA
			x	y	z			
<0.001	955	5.88	34	−28	58	R	SM1	4
		5.02	30	−14	68	R	PMdc	6
<0.001	613	5.38	−42	−26	58	L	SM1	4
0.003	204	4.28	−2	−10	56	L	SMA	6
0.001	236	4.68	−54	−26	12	L	GTs	41
<0.001	521	5.05	−16	−54	−18	L	Cerebellum	
<0.001	338	4.15	26	−58	−22	R	Cerebellum	

Note: GTs, superior temporal gyrus. $P < 0.05$ corrected at the cluster level.

Table 3
Brain regions activated in parallel–mirror contrast

Cluster *P*	Cluster size	Voxel *Z*	MNI coordinates			Side	Location	BA
			x	*y*	*z*			
<0.001	444	3.75	−4	2	60	L	Pre-SMA	6
		3.61	6	4	60	R	Pre-SMA	6
		3.5	8	−8	62	R	SMA	6
		3.52	10	0	38	R	CCZ	24
0.002	298	4.39	−30	−20	60	L	SM1	4
		4.29	−30	−12	58	L	PMdc	6
0.003	269	4.22	34	−14	54	R	PMdc	6
0.009	199	4.27	32	−44	54	R	LPi	40
0.017	161	3.37	46	−2	12	R	Insula	13
0.045	103	4.09	−54	2	26	L	PMv	6
<0.001	837	6.06	24	−10	0	R	Globus pallidus	
		5.09	24	10	2	R	Putamen	
		3.96	10	−10	16	R	Thalamus	
<0.001	465	5.18	−22	−12	2	L	Globus pallidus	
		4.77	−22	0	2	L	Putamen	
		3.24	−14	−16	18	L	Thalamus	
<0.001	2273	5.38	4	−54	−18	R	Cerebellar vermis	
		5.1	28	−46	−30	R	Cerebellum	
		4.29	−34	−52	−28	L	Cerebellum	

Note: $P < 0.05$ corrected at the cluster level.

Table 4
Brain regions activated in phase-transition contrast

Cluster *P*	Cluster size	Voxel *Z*	MNI coordinates			Side	Location	BA
			x	*y*	*z*			
<0.001	12 649	4.92	10	18	60	R	Pre-SMA	6
		3.62	−8	14	58	L	Pre-SMA	6
		3.52	24	12	58	R	PMdr	6
		4.38	44	2	44	R	PMv	6
		4.14	10	36	26	R	RCZ	32
		4.41	−8	14	44	L	RCZ	32
		5.2	58	12	24	R	GFi	45
		4.38	32	48	−4	R	GFm	10
		5.35	30	18	−6	R	Insula	13
		4.36	6	−24	26	R	CC	
		3.53	−8	−34	24	L	CC	
		4.12	−6	18	18	L	CC	
<0.001	2810	5.07	−40	16	0	L	Insula	13
		4.28	−54	8	20	L	GFi	44
		3.17	−40	−8	38	L	PMv	6
<0.001	3604	5.58	42	−44	54	R	LPi	40
<0.001	2224	4.7	−44	−46	46	L	LPi	40
<0.001	634	4.18	−30	42	22	L	GFm	10
<0.001	726	4.27	8	−8	0	R	Thalamus	
		4.32	−6	−12	−2	L	Thalamus	
		3.54	8	−18	−12	R	Midbrain	
<0.001	693	4.02	−18	−62	−40	L	Cerebellum	

Note: $P < 0.05$ corrected at the cluster level.

Table 5
Asymmetric activation

Cluster *P*	Cluster size	Voxel *Z*	MNI coordinates			Side	Location	BA
			x	*y*	*z*			
Phase transition								
<0.001	746	4.35	28	4	62	R	PMdr	6
		4.23	28	2	50	R	PMv	6
		4.18	54	10	22	R	GFi	44
<0.001	388	4.66	48	−32	50	R	LPi	40
0.01	71	4.04	44	46	10	R	GFm	46
0.019	61	3.92	54	−42	46	R	LPi	40
0.031	53	3.59	22	58	14	R	GFs	10
Parallel mode								
0.001	71	3.95	32	−26	54	R	SM1	4
0.05	26	3.86	32	−12	62	R	PMdc	6
0.002	65	3.67	−8	−4	70	L	SMA	6
0.03	31	4.16	−28	−56	−18	L	Cerebellum	
Mirror mode								
<0.001	137	4.47	30	−28	62	R	SM1	4
0.03	23	3.9	−52	−40	16	L	GTs	22

Note: GFs, superior frontal gyrus; GTs, superior temporal gyrus. $P < 0.05$ corrected at the cluster level.

proper and the PMdc (Fig. 3*a*). There was little overlap between the state- and transition-related activation (yellow, Fig. 3*a*). Figure 3*b* shows the activation maps of 3 typical subjects. Figure 3*c* shows the temporal profile of the brain activity of a typical subject, illustrating that the transition-related activation is distinct from the state-related activation.

Figure 4 shows transition-related activity in the CC. Individual analyses in the present study revealed that the activation in the CC was continuous with that in the medial portion of both hemispheres. This tendency was preserved in the group analysis.

By comparing the flipped image of the phase-transition contrast with the original image, we found that the transition-related activation was right lateralized (Table 5, Fig. 5*b*); this means that the brain activation during the phase transition was greater in the right cerebral hemisphere than in the left. The right-lateralized pattern did not correlate with the behavioral laterality index (Supplementary Fig. 1).

Discussion

In this study, we investigated the neural correlates of the involuntary phase transition in bimanual coordination. By setting the appropriate movement frequency for each subject, the involuntary phase transition to the mirror mode was induced after at least 10 s of parallel-mode movement. Continuous fMRI recording allowed the detection of brain activity before (parallel mode), during, and after (mirror mode) the transition. Phase-transition–related activity was found in the pre-SMA, right PMdr, and the bilateral prefrontal cortex, LPi, and RCZ. This activity was distinct from the state-related activity of the motor execution areas (Sadato and others 1997; Stephan, Binkofski, Halsband, and others 1999; Stephan, Binkofski, Posse, and others 1999; Toyokura and others 1999; Immisch and others 2001; Debaere and others 2004).

Parieto-Premotor-Prefrontal Network

Brodmann area 6 (BA6) can be segregated anatomically and functionally in the rostrocaudal direction in primates (Geyer and others 2000). The SMA proper and the PMdc in the caudal portion of BA6 have a closer relationship with M1, have direct corticospinal projections, and are involved primarily in motor execution (Murray and Coulter 1981; He and others 1993, 1995). By contrast, the pre-SMA and the PMdr are closely interconnected with the prefrontal cortex and are responsible for motor planning or preparation (Barbas and Pandya 1987; Luppino and others 1993; Lu and others 1994). The pre-SMA and PMdr are involved with the sensory components of motor tasks (Deiber and others 1991, 1997; Grafton and others 1998; Rijntjes and others 1999; Toni and others 1999). The pre-SMA is involved in somatosensory temporal discrimination and might play a role in the temporal processing of somatosensory events (Pastor and others 2004). Sensory information processing during visuomotor tasks evokes more prominent neural activity in the PMdr than in the PMdc (Weinrich and Wise 1982; Johnson and others 1996; Shen and Alexander 1997). This

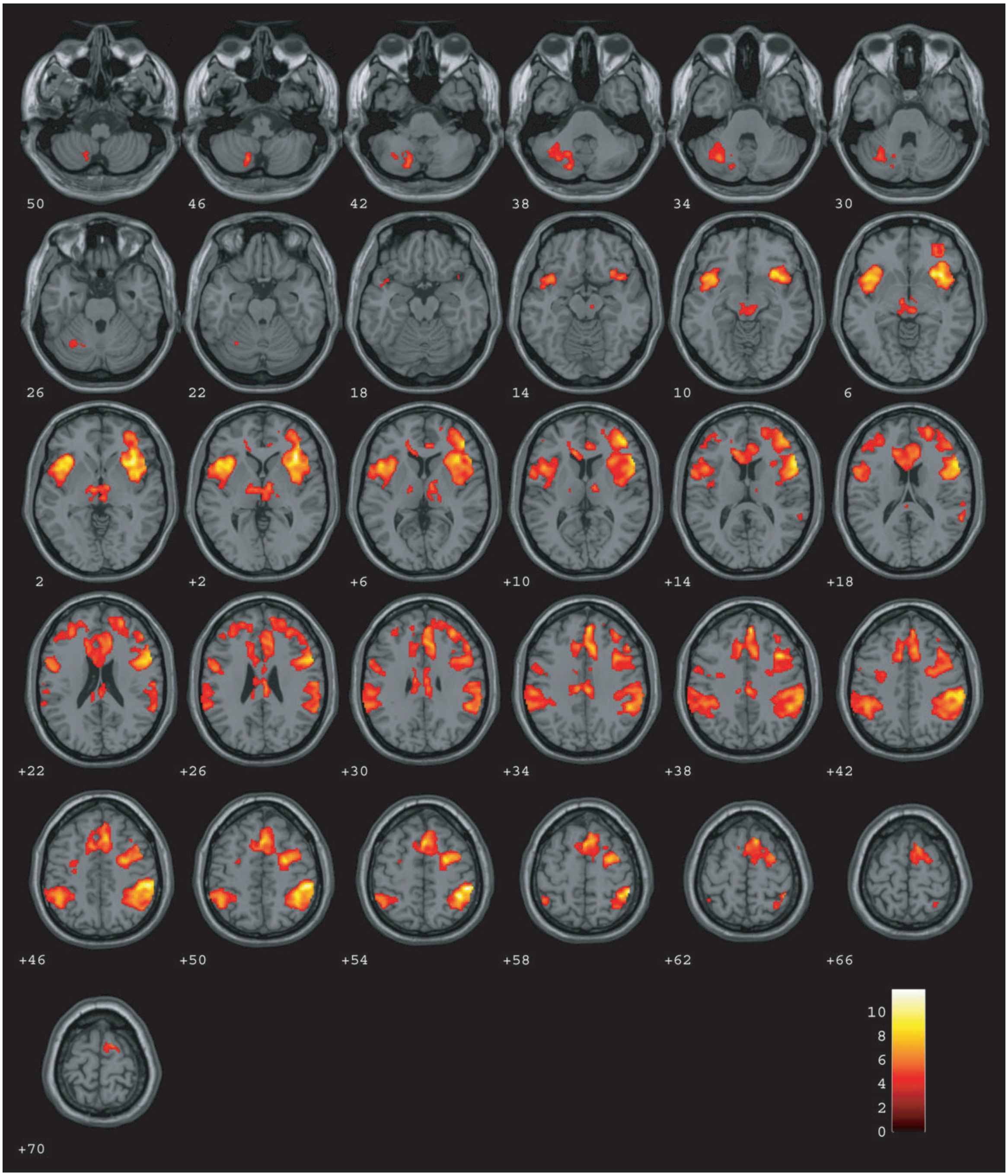

Figure 2. Statistical parametric maps of the enhanced neural activity during the spontaneous phase transition. Activated foci are shown as a pseudocolor fMRI superimposed on a high-resolution anatomical MRI in 31 contiguous transaxial planes with a 4-mm interval, extending from 50 mm below the Anterior Commissure–Posterior Commissure plane (top left) to 70 mm above the AC–PC plane (bottom left). The statistical threshold was $P < 0.05$ with a correction for multiple comparisons.

suggests that the rostral part of BA6 is crucial to the planning of perceptually guided actions.

In the present study, the bimanual movements were initially temporally stable, as both hands in the parallel mode tapped simultaneously. During the transition period, temporal stability was disturbed (Fig. 1*b*). At the same time, the spatial coordination pattern of the parallel mode was disturbed during the phase transition, and the system was subsequently restored to the more stable mirror mode. Hence, the phase transition can be viewed as the process of restoring temporal and spatial stability using tapping-associated somatosensory and proprioceptive inputs. As the pre-SMA plays a role in timing functions (Ramnani and Passingham 2001; Pastor and others 2004) and the PMd is involved in spatial functions (Wenderoth and others 2004), the pre-SMA might be related to the restoration of the temporal compatibility of the spontaneous coordination phenomenon, whereas the PMdr could be related to the restoration of the spatial compatibility of bimanual coordination.

The posterior parietal cortex (BA7/40) consists of many subdivisions, each of which is involved in particular aspects of

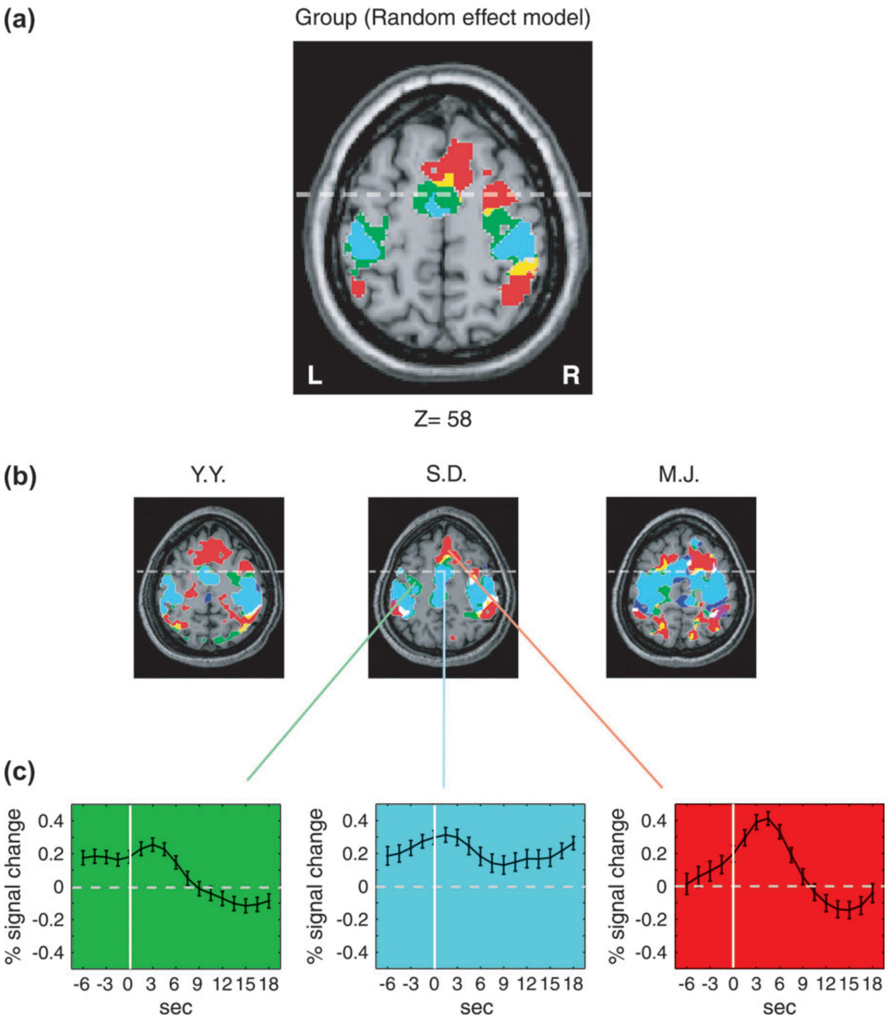

Figure 3. Activation distinctions between the mode- and transition-related conditions. (*a*) Activation map of group analysis. Areas activated by the parallel mode (green), the phase transition (red), the overlap between the parallel and mirror modes (light blue), and the phase transition and parallel mode (yellow) are superimposed on an axial view ($Z = 58$ mm in MNI coordinates) of T_1-weighted MRI scans unrelated to the subjects of the present study. To clearly illustrate the distinction between, and overlapping of, each contrast, the activation map has no intensity gradation. The statistical threshold for each contrast is $P < 0.05$ (corrected). The white dashed line indicates the AC line ($y = 0$ mm). (*b*) An individual activation map superimposed on an axial view ($Z = 58$ mm in MNI coordinates) of the T_1-weighted MRI of each individual. In addition to the contrasts shown in the group analysis, the mirror mode (dark blue), the overlap between the phase transition and parallel mode (yellow), the phase transition and mirror mode (purple), and all 3 contrasts (white) are also shown. Note that activated areas during the parallel and mirror modes are markedly overlapped, whereas transition-related activity is distinct from the activity during the state-related conditions. (*c*) The time course of the MR signal of an individual (SD). Areas activated by the parallel mode (green panel); the percentage of MR signal during the parallel mode increased compared with the rest condition and decreased after the transition (0 s; vertical white line). Areas activated by both the parallel and mirror modes (blue panel); the percentage of MR signal constantly increased compared with the rest condition. Areas activated by the phase transition (red panel) revealed a transient increase of the signal at around the phase transition without the state-related activation.

visual or somatosensory information processing. The posterior parietal cortex and BA6 are connected in specific patterns and form several frontoparietal circuits (Rizzolatti and others 1998; Geyer and others 2000). These 2 cortical areas function jointly during cognitive operations and motor control (Deiber and others 1997). The pre-SMA and frontoparietal networks between the PMdr and LPi might mediate the spontaneous phase transition.

The transition-related activation that is distinct from motor execution activation might be because our preference for mirror symmetry arises from a preference for perceptual symmetry (Mechsner and others 2001; but see also Salter and others 2004; Welsh and others 2005). Indeed, other spontaneous coordination phenomena exist, such as sensorimotor synchronization (Kelso and others 1990) and between-subject coordination (Schmidt and others 1990). The spontaneous phase transition in bimanual coordination is, however, different from other spontaneous coordination phenomena as there is a strong constraint derived from the interhemispheric anatomical coupling. Kennerley and others (2002) reported that callosotomy patients cannot perform even in-phase bimanual circle drawing, and phase transitions were observed from anti- to in-phase and vice versa, whereas controls made the transition only in the former direction. Therefore, in normal subjects, the interaction of the bilateral hemispheres through the CC is important for the enhanced stability of the in-phase movements. Anatomically, the pre-SMA has callosal connections to its contralateral counterpart and to the PMdr and PMv, which are involved in interhemispheric interaction (Liu and others 2002). Hence, the pre-SMA and PMdr might be involved in

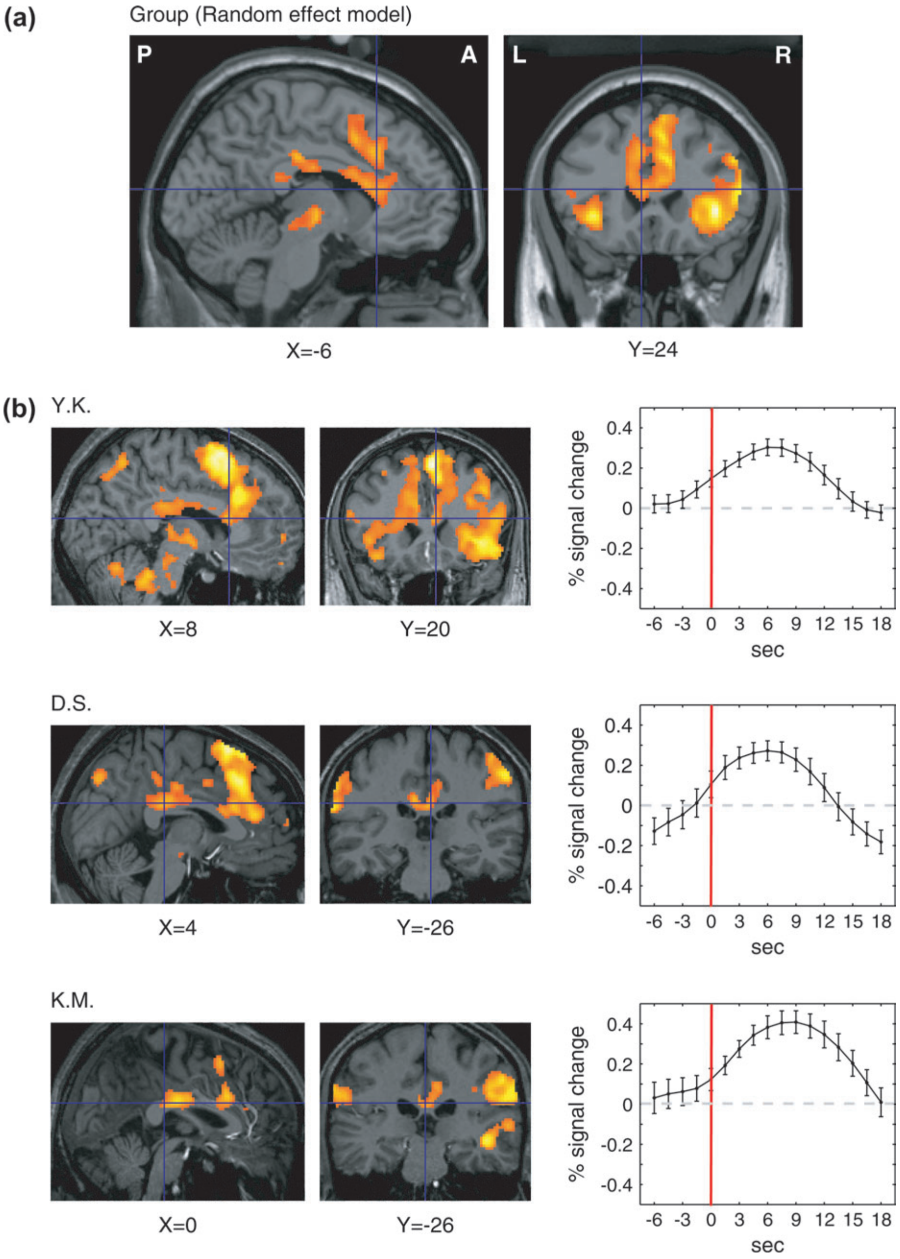

Figure 4. Phase-transition–related activity of the CC. (*a*) Statistical parametric maps of the group analysis with a random-effect model ($P < 0.05$, corrected). Transition-related increases in the MR signal superimposed on sagittal and coronal sections of T_1-weighted high-resolution MRIs unrelated to the subjects of the present study. Blue lines indicate the projections of each section that cross at the center of the genu of the CC. (*b*) Statistical parametric maps of individual analyses ($P < 0.05$, corrected). Transition-related increases in the MR signal superimposed on sagittal (left column) and coronal sections (middle column) of T_1-weighted high-resolution MRIs of each subject. Continuous activation of the bilateral medial walls of both hemispheres through the CC is noted. (Right column) The time courses of the MR signal around the phase transition (0 s; vertical red line) of the cross point of the blue lines in the activation maps.

interhemispheric interaction during the spontaneous phase transition.

Anterior Cingulate Cortex and CC

We also found transition-related activation in the RCZ (Picard and Strick 1996) extending to the CC. The RCZ is located in rostral BA24 and BA32, rostral to the CCZ in BA24 near the Vca line (a vertical line traversing the posterior margin of the anterior commissure). The CCZ in humans corresponds to the dorsal cingulate motor area (CMAd) of monkeys. The RCZ of humans is tentatively associated with the rostral cingulate motor area (CMAr) and ventral cingulate motor area (CMAv) (Picard and Strick 1996). The RCZ is involved in higher order aspects of motor behavior, whereas the CCZ is activated by somatosensory stimulation and during simple motor tasks. Callosal connections between the left and right cingulate cortex have been well documented in monkeys (Pandya and Seltzer 1986) and humans (Locke and Yakovlev 1965). The CMAr and CMAv radiate to the prefrontal cortex but not to the CMAd (Bates and Goldman-Rakic 1993). Correspondingly, an association between the activation in the RCZ and prefrontal cortex has been observed in human functional neuroimaging studies (Picard and Strick 1996). Despite the anatomical and functional differences among the various motor areas in the medial frontal

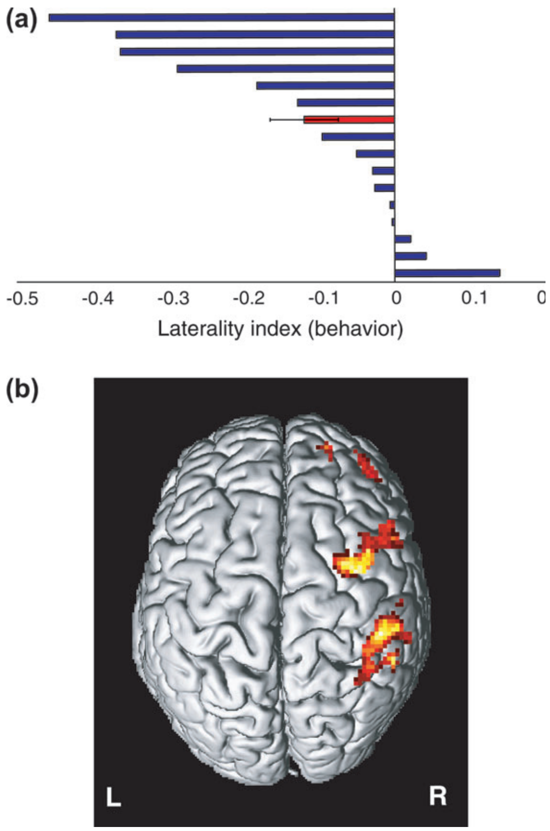

Figure 5. Laterality in behavior and brain activation. (*a*) Behavioral laterality indices for individuals (blue) and the group mean ± standard error ($n = 15$, red). A negative value means that the fluctuations in the intertap interval of the left index finger around the phase transition were greater than those of the right index finger. (*b*) The asymmetric neural representation of the transition-related activity. The contrast images of the phase transition were compared with those flipped in the horizontal (right–left) direction in a pairwise manner (corrected $P < 0.05$). The statistical parametric map was superimposed on a sample surface rendered by high-resolution MRI and is also shown in standard anatomical space.

cortex (Vogt and others 1995; Zilles and others 1995; Picard and Strick 1996), the medial frontal cortex appears to represent a functional unit that allows various medial motor areas to participate flexibly in the motor task (Stancak and others 2003). The recruitment of callosal fibers obviously contributes to the integration of the left and right medial frontal cortices capable of eliciting right or left unilateral or bilateral movements (Tanji and others 1988). Stancak and others (2003) reported that in neurologically healthy human subjects the size of the CC correlates positively with the activity registered in cingulate cortical areas during both unimanual and bimanual movements. This finding supports the existence of high-level cross talk through the nonprimary motor areas and the CC.

The CC activation during the involuntary phase transition was unexpected because white matter activation has seldom been reported in previous fMRI studies. The blood oxygenation level dependent (BOLD) signal reflects local field potentials rather than spiking (Logothetis and others 2001); as the former are caused by excitatory neurotransmission in postsynaptic extensions (dendrites), the BOLD signal changes in gray matter reflect synaptic activity (Raichle 1987). Even in white matter, however, glucose metabolism is tightly coupled with cerebral blood flow (Weber and others 2002). Hence, a task-related increase in blood flow (and a BOLD signal increase in fMRI) is possible, at least theoretically. Task-related CC activation has been reported previously (Tettamanti and others 2002). Regarding putative mechanisms of CC activation, Tettamanti and others (2002) raised several possibilities, such as the reverse transport of glutamate in axons (Chiu and Kriegler 1994) and axo-axonal coupling (Schmitz and others 2001). Although differences in perfusion, and consequently in the BOLD signal, between the rest and activation states are normally much smaller in white than in gray matter (Preibisch and Haase 2001), the increased demand for axonal communication through the CC is sufficient to induce increases in local metabolism (Tettamanti and others 2002). Therefore, the activation of the CC in this study might partly represent transient interhemispheric interaction.

Asymmetric Transition-Related Activation

We found right-dominant activity in the PMdr, LPi, and dorsolateral prefrontal cortex (DLPFC) in the phase transition condition. At the behavioral level, the spontaneous phase transition was asymmetrical, such that the left-finger tapping was attracted to the phase of the right-finger tapping. Hence, the critical question is whether the lateralized activation network is specific to phase transitions per se or if it is related to the phase transition through one particular hand. First, the behavioral laterality index is not particularly high for strongly right-handed subjects (handedness index > 0.8). This implies that the behavioral asymmetry is influenced not only by hemispheric laterality but also by other musculoskeletal factors (Byblow and others 1994). Second, there is no significant correlation between the laterality of the neural activation and the behavioral laterality index. In fact, the subjects with a tendency for the right fingers to disrupt the spatial and temporal consistency also showed the right-lateralized activation pattern; hence, the phase transition does not necessarily involve a change in the performance of the left hand. We therefore conclude that the asymmetric activation might be related to the phase transition itself.

Clinical and imaging studies have indicated left-hemisphere dominance in the representation of motor skill. Patients with ideomotor limb apraxia showed evidence of damage lateralized to a left-hemispheric network involving the GFm and the intraparietal sulcus region (Haaland and others 2000). Patients with lesions restricted to the parietal cortex were found to be selectively impaired at using mental imagery to predict the time necessary to perform differentiated finger movements and visually guided pointing gestures. This suggests that the parietal cortex is important for the ability to generate mental representations of movements (Sirigu and others 1996). Left-parietal damage led to the desynchronization of bimanual movement trajectories, and this was most apparent during the performance of parallel movement patterns (Serrien and others 2001). As the neural substrates of these examples of motor planning are left lateralized and upstream of M1, the high-level cross talk is likely to be driven from the left to the right hemisphere.

A previous electroencephalogram (EEG) study revealed that in bimanual movement the drive in the β-band frequency of the EEG from the dominant to the nondominant hemisphere prevailed (Serrien and others 2003). Right-lateralized activation in the phase transition might be related to a transient increase in the drive from left to right. As the hemodynamic response correlates with the local field potentials, the right-lateralized activation found in the present study probably reflects the incoming input and local processing (Logothetis and others 2001). Thus, the right-lateralized activity of frontoparietal areas might represent the asymmetrical interhemispheric interaction driven from left to right during the phase transition.

In summary, the present study tested the cross-talk model of bimanual coordination in order to identify the connection between large-scale brain dynamics and behavior. The neural substrates of the spontaneous phase transition during bimanual finger tapping seem to be upstream of the cortical areas for bimanual motor execution. These anatomical regions are distributed in both hemispheres, probably interacting though the CC. The transition-related activation was right lateralized, reflecting the left-lateralized common motor program. Finally, in parallel with the behavioral changes, extensive cortical involvement during the phase transition represents the characteristics of a nonlinear system, such that minute changes to the state result in large-scale alterations. Similar mechanisms might also operate in other complex movements that require coordination between their components; thus, these results contribute to our understanding of motor coordination in general.

Supplementary Material

Supplementary material can be found at: http://www.cercor.oxfordjournals.org/.

Notes

This study was supported, in part, by Grant in Aid for Scientific Research B#14380380 (NS) and S#17100003 (NS) from the Japan Society for the Promotion of Science and by Grant in Aid for Scientific Research 018#17021045 (NS) from the Ministry of Education, Culture, Sports, Science and Technology of the Japanese Government. The authors would like to thank H. Tanabe, D. Saito, and Y. Yamamoto for their help with data acquisition.

Address correspondence to Dr Norihiro Sadato, MD, PhD, Division of Cerebral Integration, Department of Cerebral Research, National Institute for Physiological Sciences, 38 Nishigonaka, Myodaijicho, Okazaki 444-8585, Japan. Email: sadato@nips.ac.jp.

Funding to pay the Open Access publication charges for this article was provided by Grant in Aid for Scientific Research S#17100003 from the Japan Society for the Promotion of Science.

References

Barbas H, Pandya DN. 1987. Architecture and frontal cortical connections of the premotor cortex (area 6) in the rhesus monkey. J Comp Neurol 256:211–228.

Bates J, Goldman-Rakic P. 1993. Prefrontal connections of medial motor areas in the rhesus monkey. J Comp Neurol 335:211–228.

Buchel C, Friston KJ. 1997. Modulation of connectivity in visual pathways by attention: cortical interactions evaluated with structural equation modelling and fMRI. Cereb Cortex 7:768–778.

Byblow WD, Bysouth-Young D, Summers JJ, Carson RG. 1998. Performance asymmetries and coupling dynamics in the acquisition of multifrequency bimanual coordination. Psychol Res 61:56–70.

Byblow WD, Carson RG, Goodman D. 1994. Expression of asymmetries and anchoring in bimanual coordination. Hum Mov Sci 13:3–28.

Byblow WD, Lewis GN, Stinear JW, Austin NJ, Lynch M. 2000. The subdominant hand increases in the efficacy of voluntary alterations in bimanual coordination. Exp Brain Res 131:366–374.

Carson RG. 2005. Neural pathways mediating bilateral interactions between the upper limbs. Brain Res Rev. Forthcoming.

Cattaert D, Semjen A, Summers JJ. 1999. Simulating a neural cross-talk model for between-hand interference during bimanual circle drawing. Biol Cybern 81:343–358.

Chiu SY, Kriegler S. 1994. Neurotransmitter-mediated signaling between axons and glial cells. Glia 11:191–200.

de Oliveira SC. 2002. The neuronal basis of bimanual coordination: recent neurophysiological evidence and functional models. Acta Psychol (Amst) 110:139–159.

Debaere F, Wenderoth N, Sunaert S, Van Hecke P, Swinnen SP. 2004. Cerebellar and premotor function in bimanual coordination: parametric neural responses to spatio-temporal complexity and cycling frequency. Neuroimage 21:1416–1427.

Deiber MP, Passingham RE, Colebatch JG, Friston KJ, Nixon PD, Frackowiak RS. 1991. Cortical areas and the selection of movement: a study with positron emission tomography. Exp Brain Res 84:393–402.

Deiber MP, Wise SP, Honda M, Catalan MJ, Grafman J, Hallett M. 1997. Frontal and parietal networks for conditional motor learning: a positron emission tomography study. J Neurophysiol 78:977–991.

Evans AC, Kamber M, Collins DL, MacDonald D. 1994. An MRI-based probalistic atlas of neuroanatomy. In: Shorvon SD, editor. Magnetic resonance scanning and epilepsy. New York: Plenum Press. p 263–274.

Friston KJ, Ashburner J, Poline JB, Frith CD, Heather JD, Frackowiak RSJ. 1995. Spatial registration and normalization of images. Hum Brain Mapp 2:165–189.

Friston KJ, Holmes AP, Poline JB, Price CJ, Frith CD. 1996. Detecting activations in PET and fMRI: levels of inference and power. Neuroimage 4:223–235.

Friston KJ, Holmes AP, Worsley KJ. 1999. How many subjects constitute a study? Neuroimage 10:1–5.

Friston KJ, Holmes AP, Worsley KJ, Poline JP, Frith CD, Frackowiak RSJ. 1995 Statistical parametric maps in functional imaging: a general linear approach. Hum Brain Mapp 2:189–210.

Garry MI, Franks IM. 2000. Reaction time differences in spatially constrained bilateral and unilateral movements. Exp Brain Res 131:236–243.

Georgopoulos AP, Schwartz AB, Kettner RE. 1986. Neuronal population coding of movement direction. Science 233:1416–1419.

Geyer S, Matelli M, Luppino G, Zilles K. 2000. Functional neuroanatomy of the primate isocortical motor system. Anat Embryol (Berl) 202:443–474.

Grafton ST, Fagg AH, Arbib MA. 1998. Dorsal premotor cortex and conditional movement selection: a PET functional mapping study. J Neurophysiol 79:1092–1097.

Haaland KY, Harrington DL, Knight RT. 2000. Neural representations of skilled movement. Brain 123:2306–2313.

Haken H, Kelso JA, Bunz H. 1985. A theoretical model of phase transitions in human hand movements. Biol Cybern 51:347–356.

Harada T, Saito DN, Kashikura K, Sato T, Yonekura Y, Honda M, Sadato N. 2004. Asymmetrical neural substrates of tactile discrimination in humans: a functional magnetic resonance imaging study. J Neurosci 24:7524–7530.

He SQ, Dum RP, Strick PL. 1993. Topographic organization of corticospinal projections from the frontal lobe: motor areas on the lateral surface of the hemisphere. J Neurosci 13:952–980.

He SQ, Dum RP, Strick PL. 1995. Topographic organization of corticospinal projections from the frontal lobe: motor areas on the medial surface of the hemisphere. J Neurosci 15:3284–3306.

Immisch I, Waldvogel D, van Gelderen P, Hallett M. 2001. The role of the medial wall and its anatomical variations for bimanual antiphase and in-phase movements. Neuroimage 14:674–684.

Johnson PB, Ferraina S, Bianchi L, Caminiti R. 1996. Cortical networks for visual reaching: physiological and anatomical organization of frontal and parietal lobe arm regions. Cereb Cortex 6:102–119.

Kakei S, Hoffman DS, Strick PL. 1999. Muscle and movement representations in the primary motor cortex. Science 285:2136–2139.

Kalaska JF, Scott SH, Cisek P, Sergio LE. 1997. Cortical control of reaching movements. Curr Opin Neurobiol 7:849–859.

Kelso JA. 1984. Phase transitions and critical behaviour in human bimanual coordination. Am J Physiol 246:R1000–R1004.

Kelso JAS, DelColle JD, Schoner G. 1990. Action-perception as a pattern formation process. In: Jeannerod M, editor. Attention and performance XIII. Hillsdale, NJ: Erlbaum. p 139–169.

Kennerley SW, Diedrichsen J, Hazeltine E, Semjen A, Ivry RB. 2002. Callosotomy patients exhibit temporal uncoupling during continuous bimanual movements. Nat Neurosci 5:376–381.

Liu J, Morel A, Wannier T, Rouiller EM. 2002. Origins of callosal projections to the supplementary motor area (SMA): a direct comparison between pre-SMA and SMA-proper in macaque monkeys. J Comp Neurol 443:71–85.

Locke S, Yakovlev P. 1965. Transcallosal connections of the cingulum of man. Arch Neurol 13:471–476.

Logothetis NK, Pauls J, Augath M, Trinath T, Oeltermann A. 2001. Neurophysiological investigation of the basis of the fMRI signal. Nature 412:150–157.

Lu MT, Preston JB, Strick PL. 1994. Interconnections between the prefrontal cortex and the premotor areas in the frontal lobe. J Comp Neurol 341:375–392.

Luppino G, Matelli M, Camarda R, Rizzolatti G. 1993. Corticocortical connections of area F3 (SMA-proper) and area F6 (pre-SMA) in the macaque monkey. J Comp Neurol 338:114–140.

Marteniuk RG, MacKenzie CL. 1980. Information processing in movement organization and execution. In: Nickerson R, editor. Attention and performance VIII. Hillsdale, NJ: Erlbaum. p 29–57.

Mechsner F, Kerzel D, Knoblich G, Prinz W. 2001. Perceptual basis of bimanual coordination. Nature 414:69–73.

Meyer-Lindenberg A, Ziemann U, Hajak G, Cohen L, Berman KF. 2002. Transitions between dynamical states of differing stability in the human brain. Proc Natl Acad Sci USA 99:10948–10953.

Murray EA, Coulter JD. 1981. Organization of corticospinal neurons in the monkey. J Comp Neurol 195:339–365.

Oldfield RC. 1971. The assessment and analysis of handedness: the Edinburgh inventory. Neuropsychologia 9:97–113.

Pandya D, Seltzer B. 1986. The topography of commisural fibers. In: Leporé F, Ptito M, Jasper H, editors. Two hemispheres-one brain: functions of the corpus callosum. New York: Alan R. Liss. p 47–63.

Pastor MA, Day BL, Macaluso E, Friston KJ, Frackowiak RS. 2004. The functional neuroanatomy of temporal discrimination. J Neurosci 24:2585–2591.

Picard N, Strick P. 1996. Motor areas of medial wall: a review of their location and functional activation. Cereb Cortex 6:342–353.

Preibisch C, Haase A. 2001. Perfusion imaging using spin-labeling methods: contrast-to-noise comparison in functional MRI applications. Magn Reson Med 46:172–182.

Raichle ME. 1987. Circulatory and metabolic correlates of brain function in normal humans. In: Mountcastle VB, Plum F, Geiger SR, eds. Handbook of physiology. Bethesda, MD: American Physiological Society. p 643–674.

Ramnani N, Passingham RE. 2001. Changes in the human brain during rhythm learning. J Cogn Neurosci 13:952–966.

Rijntjes M, Dettmers C, Buchel C, Kiebel S, Frackowiak RS, Weiller C. 1999. A blueprint for movement: functional and anatomical representations in the human motor system. J Neurosci 19:8043–8048.

Rizzolatti G, Luppino G, Matelli M. 1998. The organization of the cortical motor system: new concepts. Electroencephalogr Clin Neurophysiol 106:283–296.

Rogers MA, Bradshaw JL, Cunnington RC, Phillips JG. 1998. Inter-limb coupling in coordinated bimanual movement: attention and asymmetries. Laterality 3:53–75.

Rose G, Siebler M. 1995. Cooperative effects of neuronal ensembles. Exp Brain Res 106:106–110.

Sadato N, Yonekura Y, Waki A, Yamada H, Ishii Y. 1997. Role of the supplementary motor area and the right premotor cortex in the coordination of bimanual finger movements. J Neurosci 17:9667–9674.

Salter JE, Wishart LR, Lee TD, Simon D. 2004. Perceptual and motor contributions to bimanual coordination. Neurosci Lett 363:102–107.

Schmidt RA. 1975. A schema theory of discrete motor skill learning. Psychol Rev 82:225–260.

Schmidt RC, Carello C, Turvey MT. 1990. Phase transitions and critical fluctuations in the visual coordination of rhythmic movements between people. J Exp Psychol Hum Percept Perform 16:227–247.

Schmitz D, Schuchmann S, Fisahn A, Draguhn A, Buhl EH, Petrasch-Parwez E, Dermietzel R, Heinemann U, Traub RD. 2001. Axo-axonal coupling: a novel mechanism for ultrafast neuronal communication. Neuron 31:831–840.

Schöner G, Kelso JA. 1988. Dynamic pattern generation in behavioral and neural systems. Science 239:1513–1520.

Semjen A, Summers JJ, Cattaert D. 1995. Hand coordination in bimanual circle drawing. J Exp Psychol Hum Percept Perform 21:1139–1157.

Serrien DJ, Cassidy MJ, Brown P. 2003. The importance of the dominant hemisphere in the organization of bimanual movements. Hum Brain Mapp 18:296–305.

Serrien DJ, Nirkko AC, Lovblad KO, Wiesendanger M. 2001. Damage to the parietal lobe impairs bimanual coordination. Neuroreport 12:2721–2724.

Shen L, Alexander GE. 1997. Preferential representation of instructed target location versus limb trajectory in dorsal premotor area. J Neurophysiol 77:1195–1212.

Sherwood DE. 1994. Hand preference, practice order, and spatial assimilations in rapid bimanual movement. J Mot Behav 26:123–134.

Sirigu A, Duhamel JR, Cohen L, Pillon B, Dubois B, Agid Y. 1996. The mental representation of hand movements after parietal cortex damage. Science 273:1564–1568.

Stancak A, Cohen ER, Seidler RD, Duong TQ, Kim SG. 2003. The size of corpus callosum correlates with functional activation of medial motor cortical areas in bimanual and unimanual movements. Cereb Cortex 13:475–485.

Stephan K, Binkofski F, Halsband U, Dohle C, Wunderlich G, Schnitzler A, Tass P, Posse S, Herzog H, Sturm V, Zilles K, Seitz R, Freund H. 1999. The role of ventral medial wall motor areas in bimanual coordination. Brain 122:351–368.

Stephan KM, Binkofski F, Posse S, Seitz RJ, Freund HJ. 1999. Cerebral midline structures in bimanual coordination. Exp Brain Res 128:243–249.

Swinnen SP, Jardin K, Meulenbroek R, Dounskaia N, Hofkens-van den Brandt M. 1997. Egocentric and allocentric constraints in the expression of patterns of interlimb coordination. J Cogn Neurosci 9:348–377.

Talairach J, Tournoux P. 1988. Co-planar stereotaxic atlas of the human brain. New York: Thieme.

Tanji J, Okano K, Sato K. 1988. Neuronal activity in cortical motor areas related to ipsilateral, contralateral, and bilateral digit movements of the monkey. J Neurophysiol 60:325–340.

Tettamanti M, Paulesu E, Scifo P, Maravita A, Fazio F, Perani D, Marzi CA. 2002. Interhemispheric transmission of visuomotor information in humans: fMRI evidence. J Neurophysiol 88:1051–1058.

Toni I, Schluter ND, Josephs O, Friston K, Passingham RE. 1999. Signal-, set- and movement-related activity in the human brain: an event-related fMRI study. Cereb Cortex 9:35–49.

Toyokura M, Muro I, Komiya T, Obara M. 1999. Relation of bimanual coordination to activation in the sensorimotor cortex and supplementary motor area: analysis using functional magnetic resonance imaging. Brain Res Bull 48:211–217.

Treffner P, Turvey M. 1995. Handedness and the asymmetric dynamics of bimanual rhythmic coordination. J Exp Psychol Hum Percept Perform 21:318–333.

Vogt B, Nimchinsky E, Vogt L, Hof P. 1995. Human cingulate cortex: surface features, flat maps, and cytoarchitecture. J Comp Neurol 359:490–506.

Walter CB, Swinnen SP. 1992. Adaptive tuning of interlimb attraction to facilitate bimanual dissociation. J Mot Behav 24:95–104.

Weber B, Fouad K, Burger C, Buck A. 2002. White matter glucose metabolism during intracortical electrostimulation: a quantitative [(18)F] fluorodeoxyglucose autoradiography study in the rat. Neuroimage 16:993–998.

Weinrich M, Wise SP. 1982. The premotor cortex of the monkey. J Neurosci 2:1329–1345.

Welsh TN, Almeida QJ, Lee TD. 2005. The effect of postural stability and spatial orientation of the upper limbs on interlimb coordination. Exp Brain Res 161:265–275.

Wenderoth N, Debaere F, Sunaert S, Van Hecke P, Swinnen SP. 2004. Parieto-premotor areas mediate directional interference during bimanual movements. Cereb Cortex 14:1153–1163.

Zilles K, Schlaug G, Matelli M, Luppino G, Schleicher A, Qu M, Dabringhaus A, Seitz R, Roland P. 1995. Mapping of human and macaque sensorimotor areas by integrating architectonic, transmitter receptor, MRI and PET data. J Anat 187:515–537.